AMERICAN ACADEMY OF OPHTHALMOLOGY®

Transplant of Induced Pluripotent Stem Cell–Derived Retinal Pigment Epithelium Strips for Macular Degeneration and Retinitis Pigmentosa

Daiki Sakai, MD,[1,2,3] Michiko Mandai, MD, PhD,[1,2] Yasuhiko Hirami, MD, PhD,[1,2] Midori Yamamoto, BA,[1] Shin-ichiro Ito, MD, PhD,[1,2] Saori Igarashi, MD,[1,2] Satoshi Yokota, MD, PhD,[1,2] Hirofumi Uyama, MD, PhD,[1,2] Masashi Fujihara, MD, PhD,[1,2] Akiko Maeda, MD, PhD,[1,2] Motoki Terada, BS,[1,4] Mitsuhiro Nishida, MS,[1,4] Yumiko Shibata, MS,[1,4] Naoko Hayashi, MS,[1] Kyoko Iseki, MA,[1,4] Takuya Miura, MS,[1] Keisuke Kajita, MD, PhD,[1,5] Masaaki Ishida, MD, PhD,[1,6] Sunao Sugita, MD, PhD,[1] Tadao Maeda, MD, PhD,[1,4] Masayo Takahashi, MD, PhD,[1,4] Yasuo Kurimoto, MD, PhD[1,2]

Purpose: To explore the safety and efficacy of the allogeneic induced pluripotent stem cell (iPSC)–derived retinal pigment epithelium (RPE) strip transplantation for patients with RPE degeneration.

Design: Single-arm, open-label, interventional study.

Participants: Three eyes from 3 patients clinically diagnosed with RPE impairment disease; 1 patient had dry age-related macular degeneration (AMD), and remaining 2 patients had *MERTK*-associated retinitis pigmentosa.

Intervention: Allogeneic iPSC-derived RPE strip transplantation was performed by a 25-gauge pars plana vitrectomy. The RPE strips were prepared by incubating iPSC-derived RPE cells in 2-mm-wide grooves in the mold. Artificial retinal detachment was generated using a 38-gauge subretinal cannula, and the RPE strips were injected into the retinal bleb using a 31-gauge cannula with the maximum graft dose limited to 2 strips.

Main Outcome Measures: The reduction of RPE abnormal area by the engraftment of transplanted allogeneic iPSC-derived RPE cells, which was measured by analyzing fluorescein angiography with an automated evaluation program at pretransplantation and up to 52 weeks posttransplantation.

Results: The primary endpoint of reducing abnormal areas of RPE through the survival of the transplanted graft cells was achieved in all patients at 52 weeks posttransplantation. Visual function assessments confirmed significant vision-related quality of life improvement and potential retinal sensitivity restoration in 1 patient with dry AMD. The successful subretinal delivery of the iPSC-derived RPE strips was confirmed during and immediately after surgery. The engraftment of RPE cells migrated out from the strips was observed using polarization-sensitive OCT specifically and visualized as characteristic hexagonal cells via adaptive optics imaging in all patients. While no serious adverse events occurred, suspected immune reactions to graft cells and epiretinal membrane formation were observed in 1 patient each.

Conclusions: A decrease in the RPE abnormal area by reliable delivery of allogeneic iPSC-derived RPE strips was achieved in all 3 cases with no serious adverse events. Further long-term studies and larger cohorts with better preoperative vision are warranted to evaluate the safety and efficacy of RPE strip transplantation.

Financial Disclosure(s): Proprietary or commercial disclosure may be found in the Footnotes and Disclosures at the end of this article.

Supplemental material available at www.ophthalmologyscience.org.

The retinal pigment epithelium (RPE) is crucial for maintaining vision. Located between the neural retina and the choroid, the RPE forms a monolayer that is essential for the survival and functioning of photoreceptor cells.[1] Impairment of the RPE owing to aging or gene mutations lead to various sight-threatening retinal diseases, including age-related macular degeneration (AMD) and inherited retinal diseases, which are major causes of blindness in developed countries.[2] A fundamental therapeutic approach in RPE degeneration is the reconstruction of a functional RPE layer by replacing diseased RPE cells with healthy ones.

Initial challenges in RPE replacement therapy date back to the 1990s, when human fetal RPE cells were used for transplantation.[3,4] Recently, stem cell technologies, such as embryonic stem cells[5] or induced pluripotent stem cells (iPSC),[6] have provided valuable sources of RPE cells for replacement therapies. Clinically, stem cell–derived RPE cell transplantation has been applied using 2 major strategies

https://doi.org/10.1016/j.xops.2025.100770
ISSN 2666-9145/25

for graft delivery. The first strategy involves transplanting cells as a monolayer sheet with or without a scaffold.[7–9] This method ensures reliable coverage of the diseased area with the correct cell polarity; however, it requires invasive surgery including large retinotomy. The second strategy is the transplantation of cell suspension,[10,11] which is less invasive and involves the subretinal injection of graft cells. However, this method has drawbacks, such as difficulty in visualizing the graft cells during and immediately after surgery and challenges in controlled delivery to the specific target site, which may potentially lead to cell leakage into the vitreous cavity. Additionally, scattered subretinal cells can be difficult to locate until they obtain substantial pigmentation, and changes at the graft site are difficult to evaluate.

To combine the advantages of these strategies while avoiding their disadvantages, we developed the RPE strips, which are strip-like aggregates of RPE cells prepared by incubating the cells in narrow grooves.[12] We confirmed that the iPSC-derived RPE strips expanded on a culture dish with a cobblestone-like appearance while retaining the unique RPE features. After transplantation into nude rats and nonhuman primates with RPE degeneration, the RPE strip expanded with correct apical-basal polarity and successfully formed a monolayer under the retina.[12,13] The RPE strip can be transplanted using a 31-gauge subretinal cannula and is visible during and immediately after surgery, which allows us to monitor even subtle changes at the graft site during follow-up; we expect this new strategy to contribute to reliable graft delivery with reduced surgical invasion. This study aimed to explore the safety and efficacy of allogeneic iPSC-derived RPE strip transplantation in patients with RPE degeneration.

Methods

Study Design and Participants

This single-arm interventional study was approved by the Certified Special Committee for Regenerative Medicine at Osaka University and the Health Science Council of the Ministry of Health, Labor and Welfare of Japan (jRCTa050210178). Written informed consent was obtained from all patients, and the study adhered to the tenets of the Declaration of Helsinki. Three patients who met the following criteria were included: (1) a clinical diagnosis of RPE impairment disease, (2) presence of a window defect observed by fluorescein angiography (FA), and (3) best-corrected visual acuity (BCVA) (decimal) of $\leq$0.3, visual field within 20° in radius as measured using Goldmann perimetry (V4-isopter), or an Esterman visual field test score of $\leq$70 points. The complete inclusion and exclusion criteria are listed in Table S1 (available at www.ophthalmologyscience.org). In this study, we defined RPE impairment disease as a retinal condition characterized by an RPE abnormality, specifically a window defect (bright choroidal hyper fluorescence seen early in the FA through diseased RPE unable to block physiological fluorescent leakage from the choroid) covering the macular area. Accompanying findings in RPE impairment disease include atrophic or exudative lesions, intraretinal or subretinal hemorrhage, RPE tears, and retinal drusen.

Primary Endpoint

The primary endpoint was the reduction of the RPE abnormal area by engraftment of transplanted allogeneic iPSC-derived RPE cells. The RPE abnormal area was measured by analyzing FA findings with an automated evaluation program before and up to 52 weeks posttransplantation. We used a modified version of the reported 2-step software that allows for objective quantification of changes in the RPE abnormal area in early-phase FA images obtained from the confocal scanning laser ophthalmoscope system (Spectralis; Heidelberg Engineering) at 30° × 30° (approximately 9 mm × 9 mm).[14] The FA images for this assessment were selected based on 2 criteria: (1) early-phase images (within 1 minute) and (2) images best depicting the transplantation area. The image registration process in the program converted the FA images to 496 pixels × 496 pixels 8-bit images. The first step involves extracting abnormal regions based on deep learning–based discrimination, followed by scoring binarized abnormal areas in pixels within the extracted region. The region of interest (ROI) was set to include 10 000 pixels (approximately 3.29 mm^2) of the transplanted area for 1 strip in FA images at 12 weeks posttransplantation by matching the location to the pigmented areas on the fundus photographs, defined as the treated zone. The image selection and ROI setting processes were carried out based on the consensus of 3 researchers (D.S., M.M., and M.Y.). The primary endpoint was considered achieved if the abnormal area within the treated zone was reduced at 52 weeks posttransplantation compared with that at pretransplantation. The automated evaluation program analyzed the same ROI on serial FA images obtained at pretransplantation and posttransplantation for each patient. The reductions in abnormal areas due to reasons other than the engraftment of transplanted cells, such as hemorrhage or scarring, were excluded. Additionally, we set ROIs in the RPE abnormal region not containing the transplanted area at 12 weeks posttransplantation and defined them as abnormal control zones for exploratory reasons.

Secondary Endpoints

The secondary endpoints included the preservation or recovery of visual function and the safety of the RPE strip and treatment procedures. Visual function was evaluated by assessing microperimetry, visual acuity, and vision-related quality of life. If microperimetry was not feasible, we performed full-field stimulus testing using an Espion system with a ColorDome LED full-field stimulator, (Diagnosys LLC), monitor tests (Metropsis, Cambridge Research Systems), and letter recognition tests. Specific protocols for each test are described later.

Graft Preparation

The allogeneic iPSC-QHJI01s04 line was established by the iPSC Stock Project organized and provided by the CiRA foundation. Clinical-grade RPE cells had been manufactured from this iPSC line in our previous clinical study, and the same stock was used for the current study.[11] The RPE strips were prepared at the cell processing center of Kobe City Eye Hospital,[15] as previously described.[12] The frozen stock of RPE cells was thawed and plated at 1×10^6 cells/well in 12-well plates coated with iMatrix 511 (#892005; Nippi. Inc) at an RPE adhesion medium maintenance ratio of 1:1 (Table S2, available at www.ophthalmologyscience.org). The next day, the medium was changed to a maintenance medium containing 10 ng/mL basic fibroblast growth factor and 0.5 μM SB431542, and cells were cultivated for 12 to 15 days with medium changes every 2 to 3 days, either manually (cases 2 and 3) or using the Maholo culture robot (case 1).[16]

For RPE strip preparation, 2-mm-wide grooves in the mold were prewetted with 20 to 30 μL of RPE maintenance medium containing 5-μM Y-27632. Retinal pigment epithelium cells (2.0×10^5 cells/groove) were seeded in each groove and incubated for 2 days in 30 to 40 μL of RPE maintenance medium containing

5-μM Y-27632. Five RPE strips/mold (each containing approximately 1.5×10^5 cells/strip) were washed 3 times with 4-mL Opti-MEM without phenol red (#11058021; Thermo Fisher Scientific Inc) and stored in a 6:1 solution of Opti-MEM with Y-27632 (final concentration of 10 μM) (FUJIFILM Wako Pure Chemical Corporation) and Purified sodium hyaluronate and chondroitin sulfate sodium (SHELLGAN 0.5 Ophthalmic Viscoelastic Preparation; Santen Pharmaceutical Co., Ltd) on the day of surgery until the time of injection.

For quality control, we confirmed the pathogen- and virus-free status of clinical samples by sterility, mycoplasma, and endotoxin detection following the Japanese Pharmacopoeia and Japanese Society for Regenerative Medicine guidelines. Cell viability in the final RPE strip was >90%. The ingredients of the culture medium are listed in Table S2.

Surgical Procedures

Pars plana vitrectomy was performed using a 25G Constellation system (Alcon Laboratories Inc), followed by posterior vitreous detachment. Artificial retinal detachment was carefully generated at the target site with Opti-MEM (Thermo Fisher Scientific Inc) containing 10-μM Y-27632, using a 38G subretinal cannula (3219 Polytip cannula 25 g/38 g; MedOne Surgical Inc). Subretinal injection of Opti-MEM was well tolerated in our previous preclinical nonhuman primate studies (Fig S1, available at www.ophthalmologyscience.org). Next, the injection hole was enlarged slightly using a gently circular movement to insert a 31G tip. A drainage puncture hole was created near the base of the retinal bleb opposite the insertion site. The iPSC-derived RPE strips, loaded with approximately 3 μL of viscoelastic media (×7 Viscoat 0.5, Alcon Japan in Opti-MEM), were gently injected into the retinal bleb using a 31G MedOne cannula with the maximum graft dose limited to 2 strips/target site. Subretinal fluid was carefully drained from the puncture with the aid of perfluorocarbon liquid. This was followed by fluid−gas exchange and subsequent replacement with silicone oil (SILICON 1000; Alcon Japan). At the end of the surgery, an intravitreal injection of 4-mg triamcinolone acetonide (MaQaid; Wakamoto) was administered. Patients were instructed to maintain a prone position for several days postsurgery, and the planned surgical removal of silicone oil was performed 1 to 2 months after the transplantation surgery using 25G pars plana vitrectomy.

Concomitant Treatments

To suppress immune reactions posttransplantation, the patients were orally administered 3-mg/kg cyclosporine (Neoral; Novartis) per day for the initial 24 weeks posttransplantation. If the 6 HLA gene loci (HLA-A, B, C, DRB1, DQB1, DPB1) of the patient matched those of the iPSC-RPE strips, subtenon or intravitreal steroid injections were scheduled at 8, 16, 24, 32, 40, and 48 weeks posttransplantation, instead of oral cyclosporine. Blood examinations at 4, 12, and 24 weeks posttransplantation were performed to maintain cyclosporine trough levels between 50 and 200 ng/mL. Additionally, patients received 0.5% moxifloxacin (Begamox; Novartis) and 0.1% betamethasone (Rinderon; Shionogi) eye drops 4 times per day for 52 weeks posttransplantation. If patients had significant cataracts, cataract extraction was performed at least 28 days prior to transplantation.

Microperimetry

Retinal sensitivity was assessed using MP-3 with the 10-2 grid (Nidek). Improvement was considered significant if the treated area showed enhancement higher than that of the abnormal control area. If direct comparison was not feasible, changes in retinal sensitivity before and after transplantation in the treated eye were compared to those in the untreated eye.

Full-Field Stimulus Testing

The full-field stimulus testing was performed using an Espion system in a completely dark room.[17] The patients were dark-adapted for 45 minutes, and their pupils were dilated with mydriatic eye drops. Both eyes were independently examined with the nontested eye shielded. Blue (448 nm), white (590 nm), green (530 nm), and red (627 nm) light stimuli from a ColorDome stimulator provided full-field light to the patients. The baseline intensity (0 dB) was set to 0.01 cd s/m^2. The patients used a 2-button box with yes/no buttons to indicate whether they perceived light after a beep followed by a stimulus. The Weibull function was applied to determine the actual threshold, accounting for false positives and negatives. Each eye underwent 3 trials for blue and red stimuli and 1 trial for white and green stimuli with a 2-minute interval between trials. An increase in retinal sensitivity pretransplantation and posttransplantation for any of the blue, white, green, or red stimuli was considered an improvement.

Monitor Test

The monitor test assessed visual function using 3 different methods provided by Metropsis (Cambridge Research Systems Ltd) in a dark room.

1. Motion direction: a 6-cm wide black streak on a white background either remained stationary or moved horizontally or vertically. The patients indicated motion direction by pressing one of 3 keys on a response box.
2. Spatial acuity: randomly displayed vertical and horizontal patterns with various widths of black and white streaks were shown. The patients identified the orientation of the streaks as either vertical or horizontal by pressing one of 2 keys.
3. Object localization: a 6 × 6 cm square appeared randomly at the 3-, 6-, 9-, and 12-o'clock positions. The patients reported the square's orientation by pressing the corresponding key on a 4-button response box.

The percentages of correct responses for vertical and horizontal motion directions, spatial acuity, and object localization were recorded. An improvement was noted if any 1 method showed an increase ≥10%, whereas a decrease ≥10% across all methods was considered deterioration. Tests that were not measurable during pretransplantation or posttransplantation visits were excluded from the analysis.

Letter Recognition Test

The patients were instructed to read each of the 26 letters of the alphabet that were displayed as 170-point white letters on a black background from a distance of 50 cm on a desk under standard room light conditions. The letters appeared in random order. Each patient was allowed up to 1 minute for identifying each letter. Accuracy of the responses was documented as a percentage, and a change ≥10% in correct answers was noted as either improvement or deterioration. Tests that were not measurable during pretransplantation or posttransplantation visits were excluded from the analysis.

Visual Acuity

Best-corrected visual acuity was measured using an ETDRS chart before transplantation. An improvement of at least 5 letters was

considered a significant gain. If the ETDRS chart was not feasible, BCVA was categorized as finger count and hand motion, with or without light perception. An improvement of ≥1 steps in these categories was considered a significant gain.

Visual Quality of Life

The visual quality of life was assessed using the National Eye Institute Visual Function Questionnaire-25 score.

Immune Rejection

Immune rejection, in this study, was defined as meeting all of the following 3 criteria: (1) disappearance of transplanted cells on the fundus photograph, (2) increased intraretinal and subretinal fluid on OCT, and (3) a positive lymphocyte-graft immune reaction (LGIR) in in vitro tests, where patient lymphocytes responded to the graft RPE cells after transplantation.[18,19] The LGIR results were evaluated based on the proliferation of 5 types of cells (CD4, CD8a, CD11b, CD19b, and NKG2A) in peripheral blood mononuclear cells cocultured with RPE cells. These results were compared with the data of peripheral blood mononuclear cells only. Lymphocyte-graft immune reaction was classified as positive (>3 positive results), suspected positive (2 positive results), or negative (1 or 0 positive results). In addition, serological analysis for donor-specific antibodies (DSAs) was performed as a reference.[20] Lymphocyte-graft immune reaction and DSA tests were outsourced to Sysmex Inc.

Unexpected Graft Overgrowth and Host Photoreceptor Thickness

The thicknesses of the transplanted RPE and host photoreceptor layers were measured using the caliper function on cross-sectional images from spectral domain OCT (Spectralis; Heidelberg Engineering). Unexpected graft overgrowth was defined as an increase in the transplanted RPE layer thickness ≥200 μm from the time point immediately after transplantation. The thickness of the host photoreceptor layer directly above the graft was monitored to detect potential harm to the host photoreceptors.

Safety of the Treatment Procedures

The safety of the treatment procedures was evaluated by assessing the frequency, duration, severity, and outcomes of adverse events and their potential relationship to the treatment procedures.

Exploratory Tests

Polarization-sensitive OCT (PS-OCT) (prototype PS-OCT system; Tomey) was used to assess the changes in the RPE abnormal area before and after transplantation. Polarization-sensitive OCT is a functional extension of OCT, which measures the polarization properties of ocular tissues.[21] The characteristic polarization property of ocular tissues is the depolarization by melanin in the RPE. The spatial randomness of retinal polarization is parameterized as polarimetric entropy, ranging from "0" (completely uniform, melanin-free) to "1" (completely random polarization, melanin-rich).[22] Raster-scanned images (1024 A-scans × 256 B-scans) covering 12 × 12 mm area (approximately 40° × 40°) were obtained. Retinal pigment epithelium line segmentation was automatically performed using built-in software and was manually confirmed. The entropy at the RPE level was defined as the average within 5 pixels (21.5 μm) upward from either the lower edge of the RPE or Bruch membrane. An en face PS-OCT image that extracted the entropy mapping at the RPE level was constructed for each patient.

Additionally, an adaptive optics (AO) fundus camera (rtx1; Imagine Eyes) was used to observe the transplanted RPE cells. The AO fundus camera uses AO technology to correct ocular aberrations in real time, enabling high-resolution imaging of the retinal microstructure. The AO camera uses 850-nm infrared flashes to illuminate a 4° square field and capture en face images of the retina with a transverse optical resolution of 250-line pairs/mm.[23,24] Adaptive optics fundus camera imaging of the transplanted area was performed at 12, 24, 36, and 52 weeks posttransplantation. To ensure comprehensive coverage of the specific area and its surroundings, >40 images were captured on each scheduled day. These images were then stitched together to generate a montage to observe the changes in the ROI over time with reference to OCT and fundus photographs. The best-focused images were selected by well-trained retina specialists (M.Y. and M.M.) for detailed cell observation. At 52 weeks posttransplantation, transscleral flood illumination was used for a relatively clear observation of the RPE. The transscleral flood illumination device, which attaches to the AO fundus camera (rtx1; Imagine Eyes), illuminates the retina at an oblique angle to prevent direct reflections from photoreceptors and enables the observation of the RPE cells.[25–29]

Quantification and Statistical Analysis

This study aimed to evaluate the safety and efficacy of the iPSC-derived RPE strip transplantation from a clinical perspective in a small cohort of patients with RPE degeneration. The sample size was not determined based on statistical considerations such as precision or power. We included 3 patients, and the raw data are provided in the manuscript, Figures, Tables, and Supplemental materials.

Results

Clinical Course of Each Patient

The RPE strips were prepared from the HLA homozygote iPSC-RPE cells[11] and passed the validation criteria (Fig S2, available at www.ophthalmologyscience.org). In this study, the patient HLA did not match that of the iPSC-RPE strips, and all patients received cyclosporine for the first 24 weeks posttransplantation without any side effects. No dose adjustments were needed over 24 weeks for case 1 (150 mg/day) and case 3 (200 mg/day). In case 2, the initial dose of 150 mg/day was immediately increased to 200 mg/day (4 mg/kg/day) due to a low trough level and remained stable thereafter. Case 1 involved a patient with dry AMD, whereas cases 2 and 3 involved patients with retinitis pigmentosa (RP). Genetic testing performed at our hospital identified pathogenic *MERTK* mutations in cases 2 and 3, but no potential causative genes were found in case 1.[30,31] Background profiles of each patient are summarized in Table 3. In the patients with RP (case 2 and 3), the vitreous membrane was tightly adhered to the retina. Posterior vitreous detachment was produced with a diamond scraper; however, the vitreous membrane was not completely removed. Additionally, in case 3, tight adhesion between the retina and Bruch membrane made it difficult to create retinal detachment within the vascular arcade, causing the subretinal space for transplantation to extend toward the periphery. Nevertheless, the successful subretinal delivery of the RPE strips was secured during

Table 3. Profiles of 3 Patients Who Underwent the RPE Strip Transplantation

	Case 1	Case 2	Case 3
Age at inclusion (yrs)	60	39	30
Sex	Female	Female	Male
Diagnosis	Dry AMD	RP	RP
Causative gene	Not identified	*MERTK*	*MERTK*
Gene mutations	N/A	Homozygous c.225del (p.Gly76fs)	Homozygous c.225del (p.Gly76fs)
Family history	None	None	A younger sister has RP
Age of onset (yrs)	54 yrs (visual field abnormality)	6 yrs (night blindness)	10 yrs (night blindness)
Baseline BCVA (decimal)	0.1 right eye (OD), 0.2 left eye (OS)	0.6 (OD), 0.1 (OS)	0.4 (OD), 0.03 (OS)
Study eye	OD	OS	OS
Transplantation dose	One strip	Two strips	Two strips
Adverse events requiring treatment	IOP elevation, Immune reactions (partially meet 2 out of 3 criteria for immune rejection*)	None	Macular edema associated with ERM

AMD = age-related macular degeneration; BCVA = best-corrected visual acuity; ERM = epiretinal membrane; IOP = intraocular pressure; N/A = not applicable; RP = retinitis pigmentosa; RPE = retinal pigment epithelium.
*Meeting all 3 criteria were required for diagnosing immune rejection in this study.

and after the surgery without any major surgical complications in all patients. The orientations of the transplanted strips at day 1 posttransplantation are shown in Figure S3 (available at www.ophthalmologyscience.org). Fundus changes pretransplantation and posttransplantation in 3 patients are shown in Figure 4.

Case 1

The patient with dry AMD received 1 RPE strip transplanted to the superotemporal marginal area of geographic atrophy with no intraoperative complications. Silicone oil was removed at 8 weeks posttransplantation. Figure S5 (available at www.ophthalmologyscience.org) shows the posttransplantation timeline including the management of steroid-induced intraocular pressure elevation and suspected immune reactions to graft cells. Oral cyclosporine was discontinued after 24 weeks as planned. At the 36-week posttransplantation visit, partial depigmentation of the graft RPE cells was observed, and OCT suggested cellular infiltration from the choroid at the graft site. Both LGIR and DSA tests were negative. The patient partially satisfied 2 out of the 3 criteria for immune rejection: (1) depigmentation (not full disappearance) of transplanted cells and (2) hyperreflective material (rather than fluid) at the graft site. Fundus angiography showed tissue staining indicative of cellular infiltration but no evidence of choroidal neovascularization was found. Indocyanine green angiography revealed small dark spots corresponding to the transplantation area, which may indicate inflammatory cell accumulation around the grafts (Fig S6, available at www.ophthalmologyscience.org). Although the condition did not meet the requirements for immune rejection in this study, we initiated both focal and systemic anti-inflammatory therapy, as we could not rule out immune reactions to the graft cells. The OCT findings of infiltration resolved 4 weeks after the start of anti-inflammatory therapy (40 weeks posttransplantation) and remained stable throughout the 52 weeks posttransplantation. A trend was observed toward recovery in graft area pigmentation at 52 weeks. Fundus photographs and OCT images showing changes before and after treatment for immune reactions are presented in Figure S7 (available at www.ophthalmologyscience.org). Subtenon injections of 20-mg triamcinolone were administered every 3 months to prevent relapse of immune reactions. Lymphocyte-graft immune reaction and DSA tests remained negative throughout the 52 weeks posttransplantation.

Case 2

The patient with *MERTK*-RP was transplanted with 2 RPE strips to the superior posterior pole, and silicone oil was removed after 8 weeks without complications. Concomitant treatments proceeded as planned. The results of LGIR and DSA tests at 52 weeks posttransplantation were negative.

Case 3

Two RPE strips were successfully inserted without complications to the superior posterior pole of the patient with *MERTK*-RP. Silicone oil was removed 8 weeks after transplantation. Macular edema associated with transparent unilateral epiretinal membrane (ERM) formation was detected 4 weeks posttransplantation. It was resolved after a single subtenon injection of 20-mg triamcinolone at 12 weeks and remained stable at 52 weeks. OCT images illustrating macular changes during this period are shown in Figure S8 (available at www.ophthalmologyscience.org). The LGIR test at 52 weeks posttransplantation showed a twofold increase only in the CD4-positive T cells compared with that of the controls, which was considered negative for rejection; however, a subtenon injection of 20-mg triamcinolone was administered as a precaution against potential immune reactions. The DSA test was negative at 52 weeks posttransplantation.

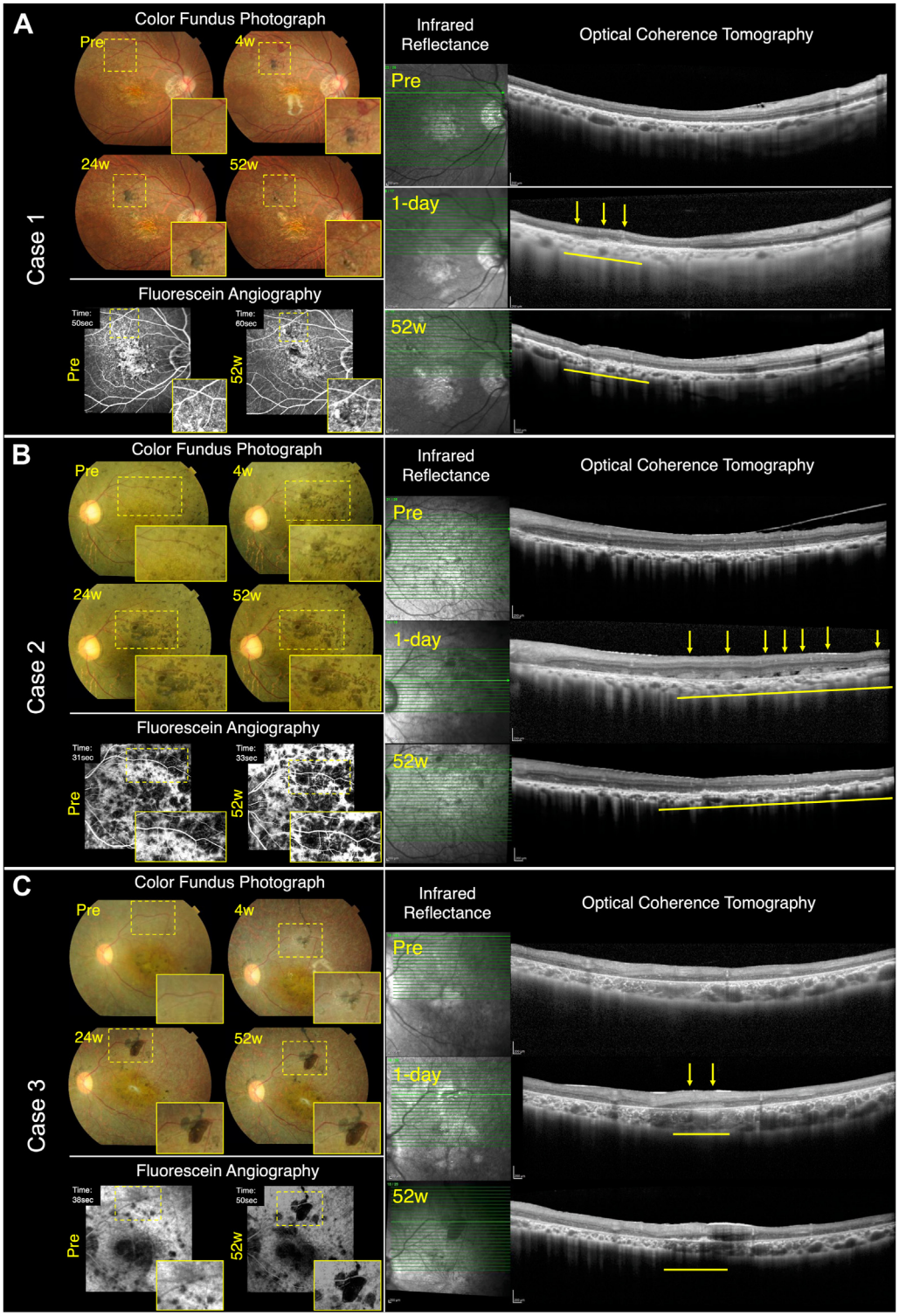

Figure 4. Multimodal fundus imaging at pretransplantation and posttransplantation. Color fundus photograph, fluorescein angiography, infrared reflectance, and OCT images pretransplantation and posttransplantation are presented for case 1 (**A**), case 2 (**B**), and case 3 (**C**); yellow dashed box: transplantation area; yellow solid box: magnified area in color fundus photograph and fluorescein angiography images. Fundus photography shows gradually increasing pigmentations in the transplantation areas after transplantation, expanding over time. In case 1, the 52 weeks posttransplantation fundus photograph presents depigmentation in the transplantation area due to immune reactions to graft cells. Fluorescein angiography shows improvements in window defects around the transplantation areas posttransplantation. Note: Magnified areas are not the same as the treated zones (See Fig S11) used for quantitative assessments of FA findings as the primary endpoint. The RPE grafts visible on the OCT images are indicated by yellow lines and yellow arrows. The strip-shaped grafts 1-day posttransplantation flatten to form the RPE-like layers at 52 weeks posttransplantation. FA = fluorescein angiography; RPE = retinal pigment epithelium.

Primary Endpoint Reduction of RPE Abnormal Area

Fluorescein angiography images taken pretransplantation and at 12, 24, and 52 weeks posttransplantation were analyzed using an automated evaluation program to measure the RPE abnormal area in pixel values. Region of interest was defined to include 10 000 pixels (approximately 3.29 mm^2) of the transplanted area for 1 strip in FA images at 12 weeks posttransplantation, which was designated as the treated zone. The control zones were established as 10 000 pixels for case 1 and 20 000 pixels for cases 2 and 3 at 12 weeks posttransplantation (Fig S9, available at www.ophthalmologyscience.org). The reproducibility of the automated evaluation program was assessed through repeated analysis of the baseline FA images (Table S4, available at www.ophthalmologyscience.org). The reduction in the RPE abnormal area from baseline for each case is summarized in Figure 10. At 52 weeks posttransplantation, the RPE abnormal areas were reduced by 0.27, 1.39, and 0.75 mm^2 for cases 1, 2, and 3, respectively (Fig S11, available at www.ophthalmologyscience.org).

Visual Function Assessment

Retinal sensitivity was measured using the 10-2 program of MP-3 in the transplanted area. In case 1, total sensitivity within the measurement area decreased from 456 dB at baseline to 438 dB at 24 weeks posttransplantation and further to 402 dB at 52 weeks posttransplantation (Fig 12). When focusing on the 15 test points within the transplanted area, subtotal sensitivity decreased from 110 dB at baseline to 66 dB at both 24 and 52 weeks posttransplantation. Immune reactions significantly influenced these results, making it difficult to evaluate the therapeutic effectiveness of RPE transplantation in this case. However, measurements covering the macular area suggested possible preservation of total sensitivity in the treated eye compared with that of the fellow eye. Assessment of therapeutic effectiveness was challenging using microperimetry in cases 2 and 3, owing to extremely low baseline retinal sensitivities and minimal changes thereafter (Fig 12).

Table 5 presents the results of other visual function assessments including BCVA (decimal and ETDRS), full-field stimulus testing, monitor test, and letter recognition test. In case 3, the treated eye consistently showed a decline across all tests, whereas visual function remained stable posttransplantation in cases 1 and 2. The Visual Function Questionnaire-25 score increased from 45.1 at baseline to 54.9 at 52 weeks posttransplantation in case 1. The scores decreased from 27.6 to 25.0 in case 2 and from 38.1 to 31.7 in case 3.

Safety of the RPE Strip and Surgical Procedures

The thicknesses of the graft RPE and host photoreceptor layers are documented in Table S6 (available at www.ophthalmologyscience.org). No signs of unexpected graft overgrowth or loss of overlying host photoreceptors were observed.

Immune reactions to graft cells were suspected in case 1, although it did not meet the study criteria for rejection (absence of intraretinal/subretinal fluid and negative LGIR result). This cellular infiltration was managed with focal and systemic anti-inflammatory therapy without complete loss of graft cells. Although focal retinal sensitivity detected using microperimetry may have been affected by immune reactions, other assessments indicated that visual function was generally preserved at 52 weeks posttransplantation.

All adverse events that could be attributed to RPE strip transplantation are listed in Table S7 (available at www.ophthalmologyscience.org). Epiretinal membrane formation was observed after transplantation surgery in case 3, accompanied by macular edema, which was managed with a focal steroid injection. Although these adverse events affected visual function, careful observation was continued to monitor and manage the outcomes.

Usefulness of Polarization-Sensitive OCT in Observing RPE Strip Transplantation

We used PS-OCT to evaluate the engraftment of RPE cells by visualizing melanin concentration in the tissues. The en face images from all 3 patients showed high-entropy areas corresponding to the expanding engraftment of transplanted iPSC-RPE beneath the retina (Fig 13). Entropy values >0.2 were extracted in reference to a previous study that analyzed RPE entropy within a 6-mm diameter circle centered on the fovea of a normal eye.[32] In addition, PS-OCT was used to assess the origin of postoperative ERM in case 3. Macular ERM was detected under silicone oil at 4 weeks post-transplantation along with epiretinal migration of graft cells around the transplantation site at 12 weeks post-transplantation. B-scan images showed low entropy on the macular surface and high entropy on the retinal surface at the transplantation site (Fig S8).

Observation of Graft RPE Cells with AO Imaging

The transplanted RPE cells were visualized using AO images at the transplantation area in all 3 cases (Fig 14). Transplanted RPE cells displayed a characteristic "bright at the border and dark at the center" appearance, similar to typical RPE images captured using an AO camera.[33] Graft RPE cells were consistently observed at the transplantation site throughout the 52 weeks, and they showed expanded engraftment. In case 2, the individual RPE morphology became somewhat blurred by the presence of uniform white dots, possibly indicating overlying photoreceptor cells. Transscleral flood illumination images at 52 weeks were obtained in 2 of the 3 cases, and RPE-like cells were observed at the transplantation site.

After detecting suspected immune reactions in case 1, AO images were captured every 4 weeks. Initially detected at 36 weeks, immune reactions seemed to decrease or blur the overall graft RPE cells. However, after 8 weeks, cells were visible again, and by 52 weeks posttransplantation,

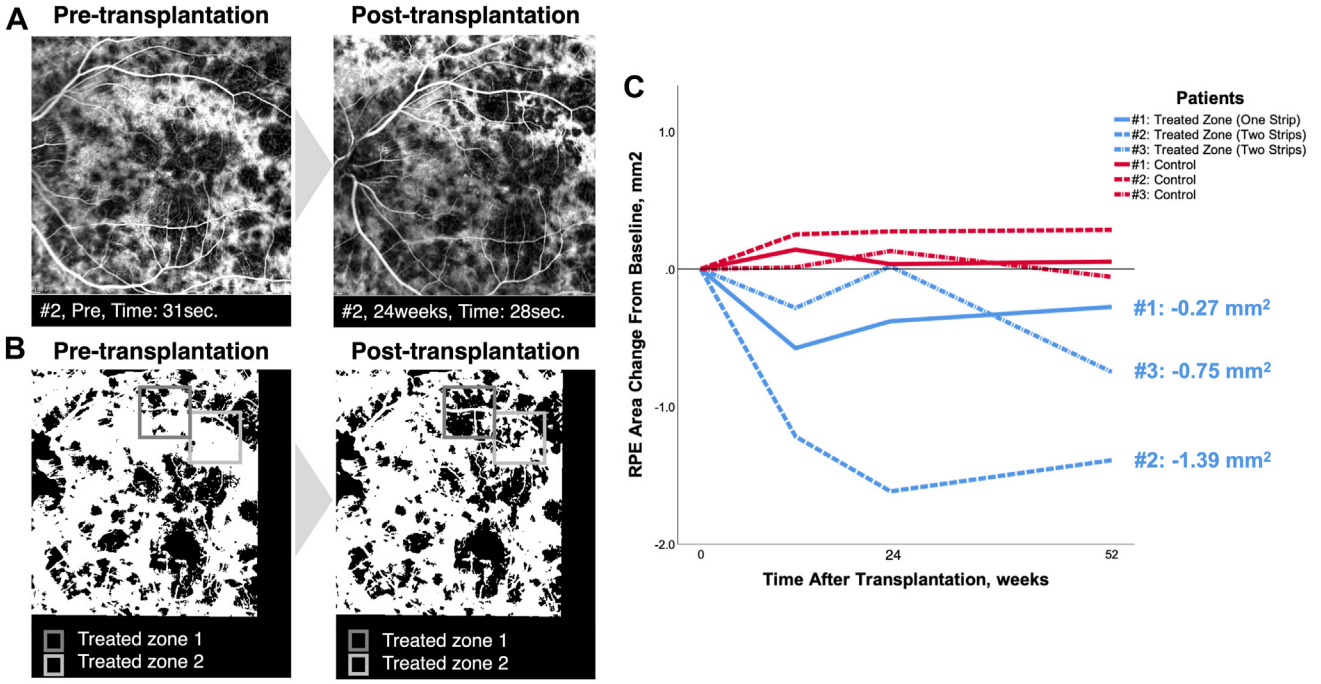

Figure 10. Reduction of RPE abnormal area. **A,** Pairwise images of early-phase fluorescein angiography at pretransplantation and 24 weeks post-transplantation in case 2. **B,** Output images obtained from analysis using automated evaluation program. **C,** Retinal pigment epithelium abnormal area reduction from baseline in 3 patients. Blue lines show changes in abnormal area in square millimeters from baseline in the treated zones, and red lines show those in the abnormal control zones. RPE = retinal pigment epithelium.

RPE cells covered the same area as before the onset of immune reactions, suggesting a trend toward recovery (Fig S15, available at www.ophthalmologyscience.org).

Discussion

This is the first clinical report of the allogeneic iPSC-derived RPE strip transplantation performed in 3 patients with RPE degeneration. The primary endpoint of reducing the RPE abnormal area through the survival of transplanted iPSC-derived RPE cells was achieved in all cases at 52 weeks posttransplantation without serious adverse events.

Our previous clinical research on RPE transplantation included 2 other methods: RPE sheet and cell suspension.[9,11] The RPE sheet transplantation closely approximates physiological conditions and potentially enhances graft function. Our prior study of autologous iPSC-derived RPE sheet transplantation in 1 case showed stable graft survival and support for overlying photoreceptors and the underlying choroid for over 4 years.[34] However, this method involves complex surgical procedures including retinotomy for subretinal graft delivery, which can lead to intraoperative complications such as retinal hemorrhage and macular holes,[35] followed by severe postoperative complications such as proliferative vitreoretinopathy.[7] The RPE cell suspension transplantation minimizes surgical invasiveness by requiring only a small injection site for subretinal delivery. In our previous study, the RPE cell suspensions were transplanted using a 38G subretinal cannula in 5 patients with AMD. However, visualizing transplanted cells during and after surgery was challenging, with a risk of continuous dispersion and backflow of graft cells into the vitreous cavity until the retina was fully reattached, which seemed to cause postoperative ERM formation. One patient developed pigmented ERM that required surgical peeling, and reverse transcription-polymerase chain reaction analysis of the removed ERM tissue indicated the presence of RPE markers such as pigment epithelium-derived factor and transforming growth factor-β2, although it contained no inflammatory cells.[11] The reported incidence of postoperative ERM by other teams varies widely from 0% to 83%.[36,37] Our molecular biological evaluation suggests that cell suspension transplantation carries a definitive risk of ERM formation originating from graft cells. Alternative approaches, such as the suprachoroidal orbit subretinal delivery system,[38] may reduce this risk; however, they introduce complications such as RPE detachment and choroidal neovascularization.[37]

We developed RPE strip transplantation as a novel technique that integrates the advantages of both the previously mentioned methods. The RPE strip can be delivered to the subretinal space through a small site using a 31G cannula, and it expands to form a physiological monolayer after transplantation.[13] This method combines the structural integrity and robust subretinal delivery of the RPE sheet with the minimally invasive nature of the RPE cell suspension. In this study, the RPE strips were securely delivered into the subretinal space without intraoperative complications in the 3 cases. The strips were visible

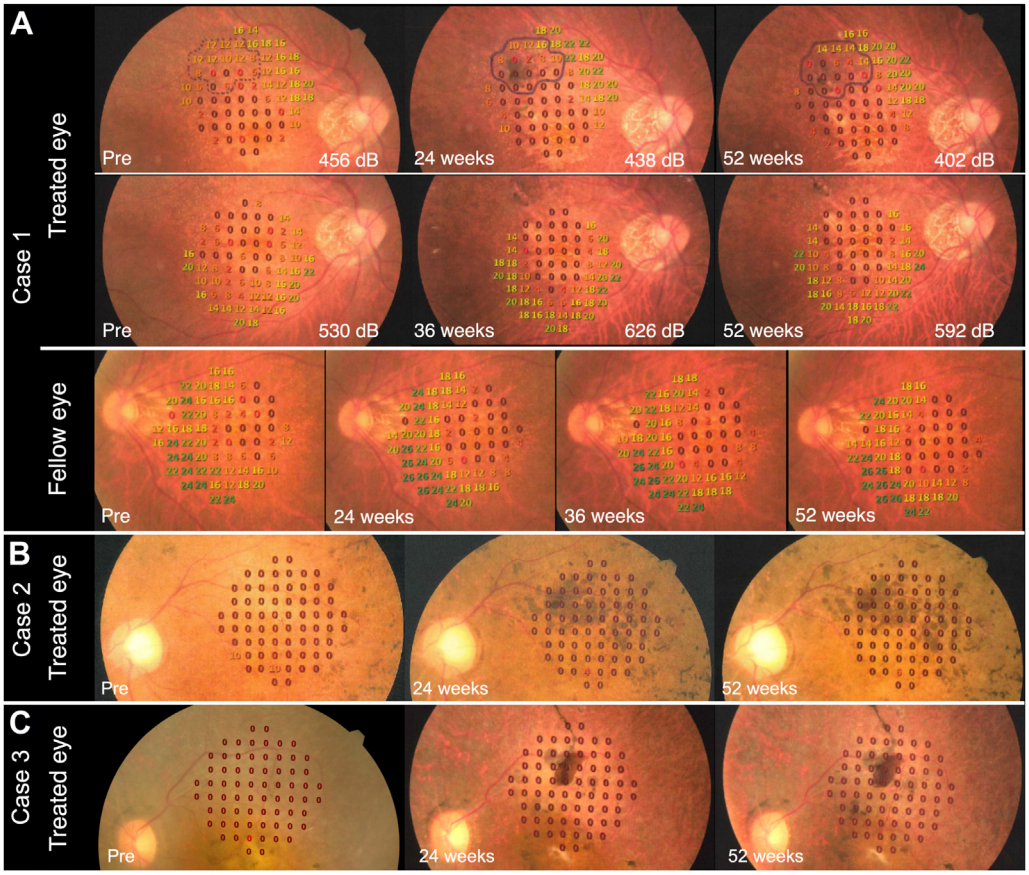

Figure 12. Visual function assessment based on retinal sensitivity measurements using microperimetry. **A,** Measurements of the transplanted area are presented on fundus photographs at pretransplantation and at 24 and 52 weeks posttransplantation in case 1. The black line surrounds 15 test points on the transplanted area. Measurements of the macular area show that total retinal sensitivity is stable at pretransplantation and 36 and 52 weeks post-transplantation in the treated eye, whereas those in the fellow eye show a gradual decrease in total sensitivity from baseline to 24, 36, and 52 weeks posttransplantation. Measurements of the transplanted area in case 2 (**B**) and case 3 (**C**) show extremely low retinal sensitivity at baseline and thereafter.

during and immediately after surgery and remained stationary until the retina was completely reattached. This stability enabled simple monitoring of graft survival during follow-up and detailed evaluations of the graft status along with any associated changes in the surrounding area, such as mild immune reactions.

We targeted patients with RPE impairment disease, which includes intractable retinal diseases primarily caused by RPE degeneration owing to aging or genetic defects, leading to secondary photoreceptor death.[39] Retinal pigment epithelium dysfunction is central to the pathophysiology of AMD and some hereditary diseases such as Bietti crystalline dystrophy, choroideremia, Best disease, and RPE with a mutation in retinoid cycle related genes such as *RPE65* and *LRAT* or phagocytosis genes such as *MERTK*.[40–46] The therapeutic concept of RPE transplantation involves the restoration of deteriorating photoreceptors by reconstructing a functional RPE layer, holding potential to preserve visual function.

Structural parameters of RPE condition have recently been used as surrogate endpoints in a clinical trial.[47] Monthly injections of pegcetacoplan, which is an inhibitor of complement protein C3, have been shown to slow the growth of RPE atrophy in patients with dry AMD by 21% at 52 weeks in the OAKS study (phase III), making it the first approved drug for dry AMD. Retinal pigment epithelium transplantation not only aims to inhibit RPE atrophy but also to reverse it. In a phase I/IIa clinical trial of subretinal RPE cell suspension transplantation (RG6501), an average improvement of 1.1 ± 2.1 mm^2 in the RPE abnormal area was observed in 12 participants.[48] Our study showed an average reduction of 2313 ± 1732 pixels (approximately 0.8 ± 0.6 mm^2) in the RPE abnormal area in 3 patients, with each participant showing a reduction. Given the initial nature of this case series, the transplantation dose was limited to 2 strips. We have confirmed the safety of up to 4 strips in animal experiments[13] and expect that future studies with higher doses will show further improvements. We performed quantitative assessment using FA images with an automated evaluation program[14] to determine RPE cell engraftment and raster scans of PS-OCT to specifically identify RPE engraftment by visualizing melanin concentration beneath the retina. Additionally, AO imaging

Table 5. Visual Function Assessments in 3 Study Participants Pretransplantation and Posttransplantation

	Case 1			Case 2			Case 3		
Visit (wks)	*Pre*	*24*	*52*	*Pre*	*24*	*52*	*Pre*	*24*	*52*
BCVA									
Decimal									
Treated	0.1	0.2	0.15	0.1	0.1	0.07	0.03	HM	0.01
Fellow	0.2	0.2	0.1	0.6	0.5	0.5	0.4	0.2	0.3
ETDRS chart (letters)									
Treated	1	2	2	6	6	4	0	0	0
Fellow	2	3	0	31	35	10	13	15	22
FST (dB)									
Blue									
Treated	−52.7	−54.5	−56.4	−0.7	−1.5	−0.3	−0.3	9.1	14.2
Fellow	−50.2	−54.2	−54.2	−4.6	−3.9	−1.3	−2.4	−0.4	3.0
White									
Treated	−44.6	−47.5	−49.5	2.3	0.9	1.4	2.0	7.6	13.7
Fellow	−46.3	−49.4	−48.4	−2.5	0.8	−0.4	−2.5	0.1	0.5
Green									
Treated	−43.2	−45.5	−46.1	0	0.2	0.8	1.5	7.1	8.3
Fellow	−46.5	−49.1	−49.4	−2.1	−1.2	−1.9	−2.1	−0.4	0.2
Red									
Treated	−29.5	−29.8	−29.4	1.5	1.4	2.4	0.6	8.4	11.5
Fellow	−25.4	−29.5	−28.6	−0.6	−0.7	−0.3	−1.8	−0.7	1.7
Monitor test (%)									
Horizontal motion direction									
Treated	94.44	94.44	100	100	100	100	100	94.44	94.44
Fellow	88.89	100	94.44	88.89	100	100	100	100	94.44
Vertical motion direction									
Treated	100	100	94.44	100	100	88.89	100	83.33	94.44
Fellow	94.44	94.44	94.44	94.44	77.78	83.33	94.44	88.89	94.44
Spatial acuity									
Treated	84.62	90.91	T85.71	82.14	100	88.89	81.48	77.78	57.14
Fellow	87.1	100	93.18	100	100	100	100	100	100
Object localization									
Treated	100	100	100	100	79.12	100	100	100	87.5
Fellow	100	100	100	100	100	100	95.83	100	100
Letter recognition test									
Treated	25/26	26/26	26/26	26/26	26/26	26/26	21/26	0/26	0/26
Fellow	26/26	26/26	26/26	26/26	26/26	26/26	26/26	26/26	26/26
VFQ-25 score	45.1		54.9	27.6		25.0	38.1		31.7

BCVA = best-corrected visual acuity; FST = full-field stimulus testing; HM = hand motion; VFQ-25 = Visual Function Questionnaire-25.

captured the expanding engraftment over time, showing a cobblestone appearance of RPE cells at the transplantation area. These multimodal imaging including innovative techniques were useful for observing the detailed behavior of grafted cells. The standard for evaluating the functionality of grafted RPE cells is currently under development. In this study, we primarily used FA to quantitatively assess the RPE abnormal area, relying on its well-established evidence and our own developed quantitative evaluation method. The following step involves comparing the FA method with less invasive imaging techniques, particularly fundus autofluorescence and OCT. Concurrently, further evidence regarding the correlation between the surrogate endpoint of RPE structural parameters and the true endpoint of visual function remains necessary.

Visual function was evaluated up to 52 weeks posttransplantation. Microperimetry was used to assess focal retinal sensitivity in the transplanted area; however, the results could only be evaluated in case 1. For cases 2 and 3, measurements showed extremely low sensitivity both pretransplantation and posttransplantation. In case 1, total sensitivity over the transplanted area declined, possibly owing to immune reactions to the graft cells; however, sensitivity in the macular area improved compared with that of the fellow eye. The patient reported noticeable improvements in recognizing specific items such as a kitchen knife and the spouse's face. This subjective visual improvement corresponded to the transplanted site even without the knowledge of the exact graft location. Additionally, an approximate 10-point increase was observed in the Visual Function Questionnaire-25 score, which assesses vision-related quality of life at 52 weeks posttransplantation from baseline. Several studies have reported potential visual function improvements following RPE transplantation, which was primarily assessed through visual acuity. A phase I clinical study of RPE sheet transplantation (NCT01691261)

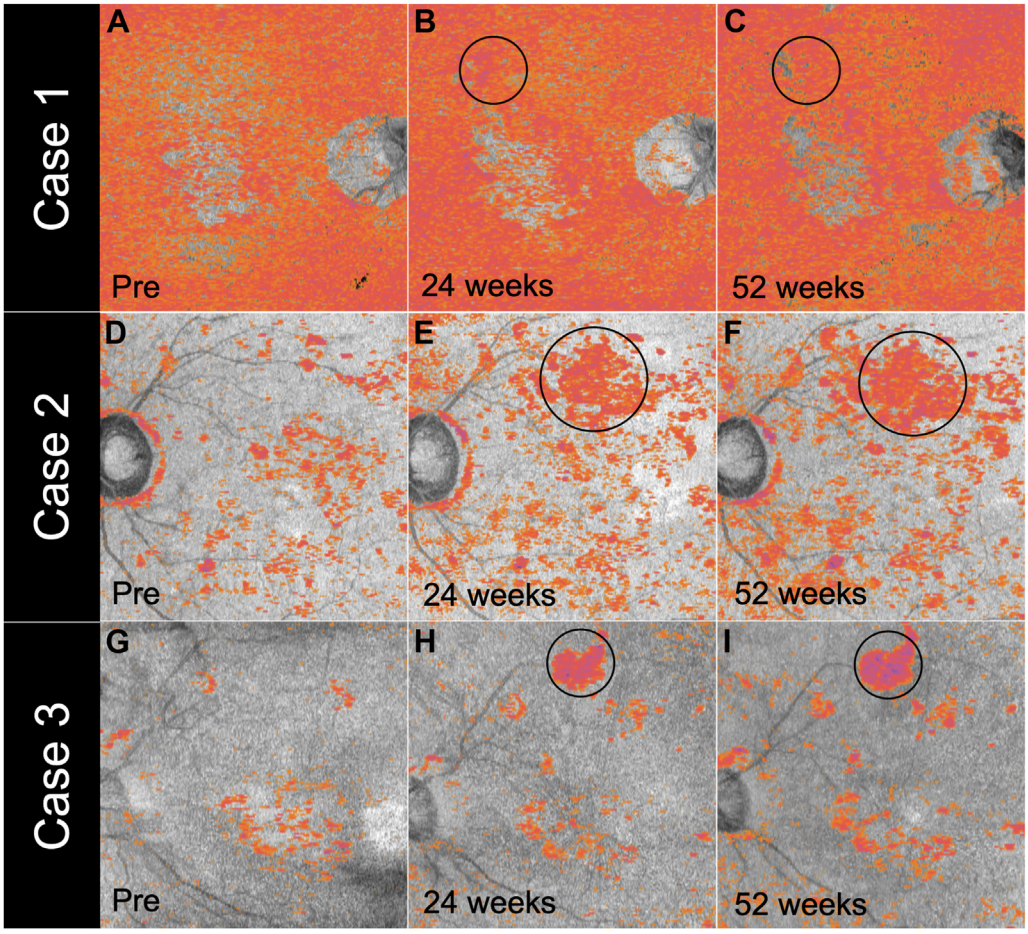

Figure 13. Usefulness of PS-OCT in observing RPE cell engraftment posttransplantation. The en face images of PS-OCT in which an entropy >0.2 was extracted at pretransplantation and at 24 and 52 weeks posttransplantation are shown for case 1 (**A**–**C**), case 2 (**D**–**F**), and case 3 (**G**–**I**). Black circles highlight the transplanted areas. PS-OCT = polarization-sensitive OCT; RPE = retinal pigment epithelium.

showed that both participants experienced an improvement of more than 15 letters.[7] However, this study included patients with active wet AMD and subretinal hemorrhage, where surgical procedures also involved subretinal hemorrhage drainage, which may have affected visual acuity recovery in addition to the sustained effect of RPE transplantation. The RG6501 phase I/IIa study of RPE cell suspension transplantation (NCT02286089) reported an average gain of 7.6 letters, with 25% of the patients gaining over 15 letters in a cohort with better preoperative visual acuity (0.08−0.3 in decimal).[37] No apparent improvement was observed in patients with worse baseline visual acuity (0.1 or less in decimal). Another study reported that at 52 weeks posttransplantation of RPE cell suspension (NCT01344993 and NCT01345006), 3 out of 7 patients with AMD and Stargardt disease had improvements of more than 15 letters.[10] Although the study included patients whose baseline BCVA ranged from 0.1 in decimal to hand motion, a subgroup analysis based on baseline BCVA was not available. In our cohort, baseline visual acuity was 0.1, 0.1, and 0.03 (decimal) for cases 1, 2, and 3, respectively, which was similar to the results of the worse cohort in the RG6501 phase I/IIa study. Future studies including patients with better preoperative visual function would help to directly evaluate the impact of RPE strip transplantation on visual outcomes.

In the current study, postoperative complications included ERM formation that occurred in 1 of the 3 cases. In case 3, the macular ERM developed at the remaining posterior vitreous, which appeared to lack melanin on PS-OCT imaging. This contrasts with the localized ERM formed by epiretinal migration of the RPE cells at graft site, or the ERM developed in our previous cell suspension clinical study, which showed melanin content both on fundus examination and PS-OCT imaging. This suggests that transparent macular ERM may have developed from an origin distinct from the RPE graft, also highlighting the importance of monitoring for the macular pucker as a potential vision-threatening complication of RPE strip transplantation performed via vitrectomy. Further histological assessment may help understand the origin of macular ERM if the surgical removal becomes necessary. Additionally, we used silicone oil tamponade to ensure clear observation of fundus changes and graft behavior immediately following transplantation.

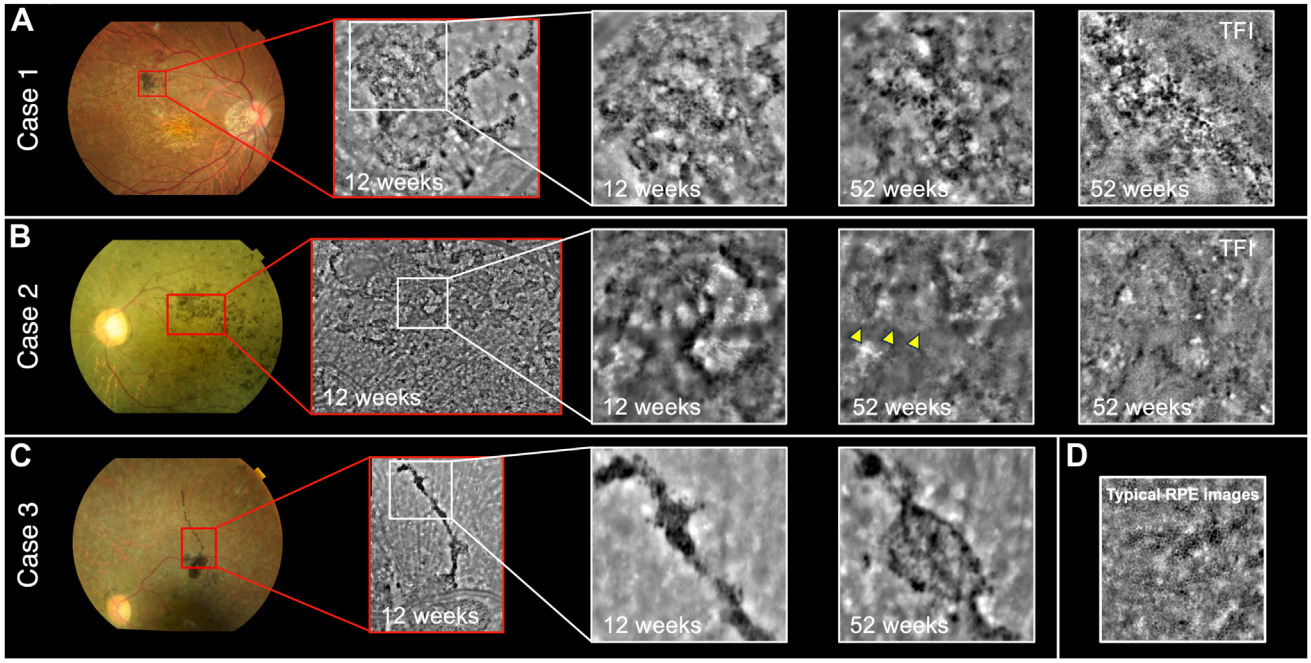

Figure 14. Graft RPE cell observation using AO imaging. Fundus photographs and adaptive optics images of transplantation areas at posttransplantation for case 1 (**A**), case 2 (**B**), and case 3 (**C**). Red squares indicate the area observed using AO imaging. White squares indicate the area of magnified images. Magnified AO images at 12 and 52 weeks posttransplantation showing expanded engraftment of RPE cells. Yellow arrow heads point to blur RPE-like findings as uniform white dots, possibly indicating overlying photoreceptors. Transscleral flood illumination images were available for cases 1 and 2. **D,** Typical RPE cell appearance captured using an AO camera with TFI in the normal eye. AO = adaptive optics; RPE = retinal pigment epithelium; TFI = transscleral flood illumination.

However, silicone oil may potentially increase the risk of ERM formation.[49] Transplantation surgery with gas tamponade would be a preferable option in the subsequent series to avoid risks of silicone oil-related complications. We observed different degrees of epiretinal migration of graft cells around the transplantation site in all cases in which melanin concentrations were detected using PS-OCT. The migrated epiretinal graft cells did not proliferate significantly and were stable at 52 weeks posttransplantation. Modifying surgical procedures, such as targeting areas distant from the retinotomy site and peeling the internal limiting membrane around the site, may mitigate the epiretinal migration of graft cells. Although we performed vitrectomy with minimized intraocular illumination while ensuring safe surgical procedures, the potential phototoxicity, particularly in cases of retinal degenerative diseases with fragile retinas, warrants further consideration. Another complication was a possible immune response owing to HLA-mismatched iPSC-derived RPE cells. Concomitant treatment including 24 weeks of oral cyclosporine administration was tolerable in all cases. One of the 3 cases showed suspected immune reactions to graft cells 12 weeks after the planned discontinuation of systemic immunosuppressants; however, systemic and focal anti-inflammatory therapies controlled immune reactions and the grafted cells survived. Although the case did not meet the protocol's criteria for immune rejection, the response to anti-inflammatory therapy served as diagnostic confirmation. This could be due to the early detection of the immune responses at the defined graft site. Both fluorescein and indocyanine green angiography supported the decision to initiate anti-inflammatory therapy. The guidelines for immune rejection may require further tuning. The results suggest that HLA-mismatched RPE transplantation could be acceptable for clinical application with careful observation, although the ideal concomitant treatment regimen for preventing immune reactions requires further discussion. Long-term use of immunosuppressants requires cautious follow-up owing to the risk of adverse events, making the use of HLA-knockout grafts a promising alternative transplant strategy.[50]

This initial case series of allogeneic iPSC-derived RPE strip transplantation involved a limited number of patients and short follow-up periods. The RPE strips were reliably delivered and engrafted to all 3 patients with RPE degeneration and decreased the RPE abnormal area assessed by FA. In animal studies, the transplanted RPE strips were most frequently placed in swirled or zigzag patterns, followed by filling of the gap spaces with migrated RPEs, as seen in case 2. In case 3, 1 of 2 strips was unexpectedly engrafted in a linear form. However, AO imaging revealed that RPE cells had migrated outward from this strip to cover a wider linear area (Fig 14). While we currently cannot control the shape of RPE engraftment, we can ensure its settled location. We believe that the surgical techniques for controlling graft shape, which may also depend on controlling how we make artificial retinal detachment at the target region, are expected to improve through the efforts of our team and other surgeons. Although no serious adverse events occurred, immune reactions to graft cells and ERM formation should be carefully monitored after transplantation surgery. Significant improvements in

vision-related quality of life and possible restoration of retinal sensitivity were observed in 1 of the 3 patients where microperimetry could be evaluated as a visual function assessment. Further investigation including long-term observations and larger patient cohorts, particularly those with better preoperative visual functions, is required for confirming the safety of RPE strip transplantation and evaluating its effectiveness in preserving visual function.

Data Availability

The data analyzed in this study and the research protocol are available from the corresponding author upon reasonable request.

Acknowledgments

The authors thank all colleagues at VCCT Inc for preparing the RPE strips; Mitsuhiro Matsuzaki at Kobe City Eye Hospital and Kota Totani and Masahiro Yamanari at Tomey corporation for supervising the analyses of polarization-sensitive OCT; Kiyoko Gocho and Elena GOFAS SALAS at Kobe City Eye Hospital for supervising the analyses of adaptive optics imaging; Noriko Sakai at VCCT Inc for preparing the RPE cells for immunological tests; Satoshi Nakadomari and Akishi Onishi at Kobe City Eye Hospital, Naohiro Motozawa at Kyoto University, Seiji Takagi at Toho University, Prof. Makoto Nakamura at Kobe University, and Prof. Jose Serafin Pulido at Wills Eye Hospital for their valuable comments; Tomoko Ito, Kanako Fujita, Kana Hatakenaka, Hidetoshi Fujiwara, Ayuko Funamoto, and Yu Sugigami at Kobe City Eye Hospital and Kenji Imoto at VCCT Inc for their valuable support for conducting this study; Tatsuo Kagimura at Translational Research Informatics Center for supervising the statistical analyses; and Prof. Hiroshi Goto at Tokyo Medical University, Prof. Motohiro Kamei at Aichi Medical University, and Prof. Akitaka Tsujikawa at Kyoto University Graduate School of Medicine for independent data monitoring. The authors also thank all colleagues of Kobe City Eye Hospital and VCCT Inc for contributing to the discussion. The clinical-grade allogeneic iPSC-QHJI01s04 line was provided by the CiRA Foundation. Audits were performed by Intellim Corporation.

Footnotes and Disclosures

Originally received: December 18, 2024.
Final revision: February 13, 2025.
Accepted: March 12, 2025.
Available online: March 18, 2025. Manuscript no. XOPS-D-24-00528.

[1] Department of Ophthalmology, Kobe City Eye Hospital, Kobe, Japan.

[2] Department of Ophthalmology, Kobe City Medical Center General Hospital, Kobe, Japan.

[3] Division of Ophthalmology, Department of Surgery, Kobe University Graduate School of Medicine, Kobe, Japan.

[4] VCCT Inc., Kobe, Japan.

[5] Department of Ophthalmology, Institute of Biomedical Sciences, Tokushima University, Graduate School, Tokushima, Japan.

[6] Department of Ophthalmology, Toyama University, Toyama, Japan.

Disclosure(s):

All authors have completed and submitted the ICMJE disclosures form.

The authors made the following disclosures:

M.M.: Consultant − VCCT Inc.

Y.H.: Consultant − VCCT Inc.; Speaker fees − Bayer, Chugai Pharmaceutical, Novartis Pharma, Santen Pharmaceuticals, Senju Pharmaceuticals.

M.T.: Employee − VCCT Inc.

M.N.: Employee − VCCT Inc.

Y.S.: Employee − VCCT Inc.

K.I.: Employee − VCCT Inc.

T.M.: Employee − VCCT Inc.

M.T.: President − VCCT Inc.

Kobe City Eye Hospital received a research grant from the Japan Agency for Medical Research and Development (AMED) (grant number: JP21bk0104118h0001) and financial support from VCCT Inc. for this study.

Support for Open Access publication was provided by Kobe City Eye Hospital.

HUMAN SUBJECTS: Human subjects were included in this study. This single-arm interventional study was approved by the Certified Special Committee for Regenerative Medicine at Osaka University and the Health Science Council of the Ministry of Health, Labor and Welfare of Japan (jRCTa050210178). Written informed consent was obtained from all patients, and the study adhered to the tenets of the Declaration of Helsinki.

No animal subjects were used in this study.

Author Contributions:

Conception and design: Sakai, Mandai, Hirami, Yamamoto, Ito, Igarashi, Yokota, Uyama, Fujihara, A. Maeda, Terada, Shibata, Sugita, T. Maeda, Takahashi, Kurimoto

Data collection: Sakai, Mandai, Hirami, Yamamoto, Ito, Igarashi, Yokota, Uyama, Fujihara, A. Maeda, Terada, Nishida, Shibata, Hayashi, Iseki, Miura, Kajita, Ishida, Sugita, T. Maeda, Takahashi, Kurimoto

Analysis and interpretation: Sakai, Mandai, Hirami, Yamamoto, Ito, Igarashi, Yokota, A. Maeda, Sugita, T. Maeda, Kurimoto

Obtained funding: N/A

Overall responsibility: Sakai, Mandai, Hirami, Yamamoto, Ito, Igarashi, Yokota, A. Maeda, Terada, Sugita, T. Maeda, Kurimoto

Abbreviations and Acronyms:
AMD = age-related macular degeneration; **AO** = adaptive optics; **BCVA** = best-corrected visual acuity; **DSA** = donor specific antibody; **ERM** = epiretinal membrane; **FA** = fluorescein angiography; **iPSC** = induced pluripotent stem cell; **LGIR** = lymphocyte-graft immune reaction; **PS-OCT** = polarization-sensitive OCT; **ROI** = region of interest; **RP** = retinitis pigmentosa; **RPE** = retinal pigment epithelium.

Keywords:
Age-related macular degeneration, iPS cells, Retinal pigment epithelium, Retinitis pigmentosa, RPE transplantation.

Correspondence:
Daiki Sakai, MD, Department of Ophthalmology, Kobe City Eye Hospitsal, 2-1-8 Minatojima Minamimachi, Chuo-ku, Kobe, Hyogo 650-0047, Japan. E-mail: dsakai1027@gmail.com; and Yasuo Kurimoto, MD, PhD, Department of Ophthalmology, Kobe City Eye Hospital, 2-1-8 Minatojima Minamimachi, Chuo-ku, Kobe, Hyogo 650-0047, Japan. E-mail: ykurimoto@me.com.

References

1. Strauss O. The retinal pigment epithelium in visual function. *Physiol Rev*. 2005;85:845–881.
2. GBD 2019 Blindness and Vision Impairment Collaborators, Vision Loss Expert Group of the Global Burden of Disease Study. Causes of blindness and vision impairment in 2020 and trends over 30 years, and prevalence of avoidable blindness in relation to VISION 2020: the Right to Sight: an analysis for the Global Burden of Disease Study. *Lancet Glob Health*. 2021;9:e144–e160.
3. Peyman GA, Blinder KJ, Paris CL, et al. A technique for retinal pigment epithelium transplantation for age-related macular degeneration secondary to extensive subfoveal scarring. *Ophthalmic Surg*. 1991;22:102–108.
4. Algvere PV, Berglin L, Gouras P, Sheng Y. Transplantation of fetal retinal pigment epithelium in age-related macular degeneration with subfoveal neovascularization. *Graefes Arch Clin Exp Ophthalmol*. 1994;232:707–716.
5. Evans MJ, Kaufman MH. Establishment in culture of pluripotential cells from mouse embryos. *Nature*. 1981;292:154–156.
6. Takahashi K, Yamanaka S. Induction of pluripotent stem cells from mouse embryonic and adult fibroblast cultures by defined factors. *Cell*. 2006;126:663–676.
7. Da Cruz L, Fynes K, Georgiadis O, et al. Phase 1 clinical study of an embryonic stem cell–derived retinal pigment epithelium patch in age-related macular degeneration. *Nat Biotechnol*. 2018;36:328–337.
8. Kashani AH, Lebkowski JS, Rahhal FM, et al. One-year follow-up in a Phase 1/2a clinical trial of an allogeneic RPE cell bioengineered implant for advanced dry age-related macular degeneration. *Transl Vis Sci Technol*. 2021;10:13.
9. Mandai M, Watanabe A, Kurimoto Y, et al. Autologous induced stem-cell–derived retinal cells for macular degeneration. *N Engl J Med*. 2017;376:1038–1046.
10. Schwartz SD, Regillo CD, Lam BL, et al. Human embryonic stem cell-derived retinal pigment epithelium in patients with age-related macular degeneration and Stargardt's macular dystrophy: follow-up of two open-label phase 1/2 studies. *Lancet Lond Engl*. 2015;385:509–516.
11. Sugita S, Mandai M, Hirami Y, et al. HLA-matched allogeneic iPS cells-derived RPE transplantation for macular degeneration. *J Clin Med*. 2020;9:2217.
12. Nishida M, Tanaka Y, Tanaka Y, et al. Human iPS cell derived RPE strips for secure delivery of graft cells at a target place with minimal surgical invasion. *Sci Rep*. 2021;11:21421.
13. Kajita K, Nishida M, Kurimoto Y, et al. Graft cell expansion from hiPSC-RPE strip after transplantation in primate eyes with or without RPE damage. *Sci Rep*. 2024;14:10044.
14. Motozawa N, Miura T, Ochiai K, et al. Automated evaluation of retinal pigment epithelium disease area in eyes with age-related macular degeneration. *Sci Rep*. 2022;12:892.
15. Terada M, Kogawa Y, Shibata Y, et al. Robotic cell processing facility for clinical research of retinal cell therapy. *SLAS Technol*. 2023;28:449–459.
16. Kanda GN, Tsuzuki T, Terada M, et al. Robotic search for optimal cell culture in regenerative medicine. *eLife*. 2022;11:e77007.
17. Klein M, Birch DG. Psychophysical assessment of low visual function in patients with retinal degenerative diseases (RDDs) with the Diagnosys full-field stimulus threshold (D-FST). *Doc Ophthalmol*. 2009;119:217–224.
18. Sugita S, Iwasaki Y, Makabe K, et al. Lack of T cell response to iPSC-derived retinal pigment epithelial cells from HLA homozygous donors. *Stem Cell Rep*. 2016;7:619–634.
19. Sugita S, Mandai M, Kamao H, Takahashi M. Immunological aspects of RPE cell transplantation. *Prog Retin Eye Res*. 2021;84:100950.
20. Sugita S, Makabe K, Fujii S, et al. Detection of retinal pigment epithelium-specific antibody in iPSC-derived retinal pigment epithelium transplantation models. *Stem Cell Rep*. 2017;9:1501–1515.
21. Pircher M, Hitzenberger CK, Schmidt-Erfurth U. Polarization sensitive optical coherence tomography in the human eye. *Prog Retin Eye Res*. 2011;30:431–451.
22. Yamanari M, Mase M, Obata R, et al. Melanin concentration and depolarization metrics measurement by polarization-sensitive optical coherence tomography. *Sci Rep*. 2020;10:19513.
23. Viard C, Nakashima K, Lamory B, et al. Imaging microscopic structures in pathological retinas using a flood-illumination adaptive optics retinal camera. *Ophthalmic Tech XXI*. 2011;7885:66–75. SPIE.
24. Lombardo M, Serrao S, Devaney N, et al. Adaptive optics technology for high-resolution retinal imaging. *Sensors (Basel)*. 2012;13:334–366.
25. Kowalczuk L, Dornier R, Kunzi M, et al. In vivo retinal pigment epithelium imaging using transscleral optical imaging in healthy eyes. *Ophthalmol Sci*. 2023;3:100234.
26. Laforest T, Künzi M, Kowalczuk L, et al. Transscleral optical phase imaging of the human retina. *Nat Photon*. 2020;14:439–445.
27. Dos Santos FLC, Laforest T, Künzi M, et al. Fully automated detection, segmentation, and analysis of in vivo RPE single cells. *Eye (Lond)*. 2021;35:1473–1481.
28. Chateau N, Rondeau C, Durand M, et al. Retinal pigment epithelium cell mosaic imaging across the macula with a modified flood-illumination adaptive optics camera. *Invest Ophthalmol Vis Sci*. 2020;61:PB00131.
29. Morgan JIW, Chui TYP, Grieve K. Twenty-five years of clinical applications using adaptive optics ophthalmoscopy [Invited]. *Biomed Opt Express*. 2022;14:387–428.
30. Maeda A, Yoshida A, Kawai K, et al. Development of a molecular diagnostic test for Retinitis Pigmentosa in the Japanese population. *Jpn J Ophthalmol*. 2018;62:451–457.
31. Sakai D, Hiraoka M, Matsuzaki M, et al. Genotype and phenotype characteristics of RHO-associated retinitis pigmentosa in the Japanese population. *Jpn J Ophthalmol*. 2023;67:138–148.
32. Fujita A, Amari T, Ueda K, et al. Three-dimensional distribution of fundus depolarization and associating factors measured using polarization-sensitive optical coherence tomography. *Transl Vis Sci Technol*. 2021;10:30.
33. Rossi EA, Chung M, Dubra A, et al. Imaging retinal mosaics in the living eye. *Eye (Lond)*. 2011;25:301–308.
34. Takagi S, Mandai M, Gocho K, et al. Evaluation of transplanted autologous induced pluripotent stem cell-derived retinal pigment epithelium in exudative age-related macular degeneration. *Ophthalmol Retina*. 2019;3:850–859.
35. Kashani AH, Uang J, Mert M, et al. Surgical method for implantation of a biosynthetic retinal pigment epithelium monolayer for geographic atrophy: experience from a phase 1/2a study. *Ophthalmol Retina*. 2020;4:264–273.

36. Schwartz SD, Tan G, Hosseini H, Nagiel A. Subretinal transplantation of embryonic stem cell-derived retinal pigment epithelium for the treatment of macular degeneration: an assessment at 4 years. *Invest Ophthalmol Vis Sci*. 2016;57: ORSFc1−ORSFc9.
37. Ho AC, Banin E, Barak A, et al. Safety and efficacy of a phase 1/2a clinical trial of transplanted allogeneic retinal pigmented epithelium (RPE, OpRegen) cells in advanced dry age-related macular degeneration (AMD). *Invest Ophthalmol Vis Sci*. 2022;63:1862.
38. Gray AP, Sato Y, Meyer T, et al. Surgical procedure and applicability of the orbit subretinal delivery system (SDS) in the normal adult canine eye. *Invest Ophthalmol Vis Sci*. 2022;63:4118. F0355.
39. Maeda T, Sugita S, Kurimoto Y, Takahashi M. Trends of stem cell therapies in age-related macular degeneration. *J Clin Med*. 2021;10:1785.
40. Hageman GS, Luthert PJ, Victor Chong NH, et al. An integrated hypothesis that considers drusen as biomarkers of immune-mediated processes at the RPE-Bruch's membrane interface in aging and age-related macular degeneration. *Prog Retin Eye Res*. 2001;20:705−732.
41. Li A, Jiao X, Munier FL, et al. Bietti crystalline corneoretinal dystrophy is caused by mutations in the novel gene CYP4V2. *Am J Hum Genet*. 2004;74:817−826.
42. Kalatzis V, Hamel CP, MacDonald IM. First international choroideremia research symposium. Choroideremia: towards a therapy. *Am J Ophthalmol*. 2013;156:433−437.e3.
43. Johnson AA, Guziewicz KE, Lee CJ, et al. Bestrophin 1 and retinal disease. *Prog Retin Eye Res*. 2017;58:45−69.
44. Kiser PD. Retinal pigment epithelium 65 kDa protein (RPE65): an update. *Prog Retin Eye Res*. 2022;88:101013.
45. Talib M, van Schooneveld MJ, van Duuren RJG, et al. Long-term follow-up of retinal degenerations associated with LRAT mutations and their comparability to phenotypes associated with RPE65 mutations. *Transl Vis Sci Technol*. 2019;8:24.
46. Feng W, Yasumura D, Matthes MT, et al. Mertk triggers uptake of photoreceptor outer segments during phagocytosis by cultured retinal pigment epithelial cells. *J Biol Chem*. 2002;277:17016−17022.
47. Heier JS, Lad EM, Holz FG, et al. Pegcetacoplan for the treatment of geographic atrophy secondary to age-related macular degeneration (OAKS and DERBY): two multicentre, randomised, double-masked, sham-controlled, phase 3 trials. *Lancet*. 2023;402:1434−1448.
48. Banin E, Barak A, Boyer DS, et al. Exploratory optical coherence tomography (OCT) analysis in patients with geographic atrophy (GA) treated by OpRegen: results from the Phase 1/2a trial. *Invest Ophthalmol Vis Sci*. 2023;64:2826.
49. Pan Q, Gao Z, Hu X, et al. Risk factors for epiretinal membrane in eyes with primary rhegmatogenous retinal detachment that received silicone oil tamponade. *Br J Ophthalmol*. 2023;107:856−861.
50. Ishida M, Masuda T, Sakai N, et al. Graft survival of major histocompatibility complex deficient stem cell-derived retinal cells. *Commun Med (Lond)*. 2024;30:187.